



## **THE HYDROSTATIC COLLAPSE PRESSURE TEST AND FAILURE ANALYSIS OF A 610 MM I.D. AS-4/APC-2 THERMOPLASTIC COMPOSITE RING-STIFFENED CYLINDER**

MARK A. LAMONTIA AND MARK B. GRUBER  
Accudyne Systems, Inc., 134 Sandy Drive, Newark, DE, USA19713

### **SUMMARY**

A 610 mm (24-inch) I.D. ring-stiffened cylinder was fabricated from AS-4/APC-2 to demonstrate its hydrostatic pressure load-carrying capability. The fabrication process was in situ thermoplastic filament winding/tape placement. Excellent laminate quality was identified by the 0.9%  $V_f$ , minimal ply undulation, uniform C-scans, and high mechanical properties measured from cylinder building blocks. The cylinder enclosed with hemispherical steel end domes was designed to exhibit a strength failure, and had a 0.212 weight-to-displacement ratio. Before testing, the team documented the expected axial collapse pressure at 39.2 MPa (5680 psi). In the test, the cylinder collapsed at 37.9 MPa (5500 psi), within 3% of prediction. Axial strains exceeded -14,000  $\mu$ strain and the shell laminate failed axially away from the hemispherical ends. The finite element model was updated with dimensions, properties, and the pre-test geometric shape resulting from process-induced residual stresses. A novel technique accounted for non-linear shear in the material constitutive law. The predicted strains matched the test strains within 15% and were often closer. Four failure criteria were evaluated using the finite element model.

### **1. INTRODUCTION**

A program to demonstrate a thermoplastic composite pressure hull model with 610 mm (24-inch) internal diameter was completed. The program goals were to

- demonstrate in situ filament winding for 90° plies and tape placement for 0° plies as a cost-effective out-of-autoclave process to fabricate the cylinder,
- achieve mechanical stiffness and strength equivalence for the thick cylindrical structure compared with compression-molded flat laminates, and
- minimize weight/displacement ratio of the cylinder.

An additional goal was to demonstrate a mid-length strength-critical failure mode in the cylinder's shell that was not significantly affected by the end closure restraints. For maximum performance, the failure would depend on a fiber-dominated strength property. The 610 mm diameter was significant for a manufacturing reason: winding back tension could not be relied upon to achieve laminate consolidation in this size cylinder (or larger). This is characteristically different from winding 178 mm (7-inch) ID or smaller cylinders where winding tension can be relied upon to achieve consolidation. All laminate consolidation was achieved with the new process [1].



## 2. CYLINDER FABRICATION AND PREPARATION FOR TEST

DuPont - Advanced Material Systems (now part of Cytec Engineered Materials) led the design and fabrication. The 610 mm (24-in) I.D., 16mm (0.629-in) wall thickness  $[90^{\circ}_{2.27/0}]_n$  APC-2/AS-4 cylinder, Figure 2.1, has five integrally wound  $90^{\circ}$  rings. The cylinder filament winding and tape placement processes [1] resulted in excellent cylinder quality [2] with 0.9% Vf, minimal ply undulation, and uniform C-scans.



Figure 2.1 The APC-2/AS-4 ring-stiffened cylinder had a  $[90^{\circ}_{2.27/0}]_n$  laminate stacking sequence and five integral  $90^{\circ}$  ring stiffeners. Quality was high with a 0.9% void volume fraction, no hoop waviness, and little axial waviness.

Cylinder fabrication followed the testing of 610 mm diameter building blocks and quantified design allowables as an integral step in fabrication process development [2]. Testing also guided the performance prediction, especially in absence of a proven failure criterion that accommodated coupled shear/compression and the multi-axial stress state. Table 2.1 lists failure pressure predictions based upon B-basis allowables. Absent an unexpected catastrophic ring fillet failure, the cylinder was predicted to collapse at 39.16 MPa (5680 psi).



Figure 3.1 In the test, the cylinder failed at 37.9 MPa (5500 psi), within 3% of prediction.

Table 2.1 Expected Failure Modes

Location	Failure Mode	MPa	Psi
<b>Shell</b>	<b>Axial Stress</b>	<b>39.2</b>	<b>5680</b>
	<i>R-Z Shear Stress</i>	50.3	7290
Shell End	<i>Axial Stress</i>	44.7	6480
<b>Ring Fillet</b>	<b><i>R-Z Shear Stress</i></b>	<b>24.7</b>	<b>3580</b>
End Closure	<i>Ultimate Stress</i>	55.7	8080
Shell	<i>General Instability</i>	58.6	8500



### 3. CYLINDER COLLAPSE TEST AND TEST OBSERVATIONS

The cylinder was tested at NSWC-CD (Naval Surface Warfare Center – Carderock Detachment). It collapsed catastrophically following external hydrostatic pressurization to 37.92 MPa (5500 psi), within 3% of prediction. Observation of the failed shell and rings indicated that an axial compression failure occurred in the shell laminate between rings 4 and 5, as shown in Figure 3.1. No evidence was found of general instability or lateral ring instability. This was corroborated by noting that axial midbay strains generally exceeded  $-14000 \mu\text{strain}$ , and hoop midbay strains were nearly equal at less than  $-7000 \mu\text{strain}$ , as shown in Figures 3.2 and 3.3.

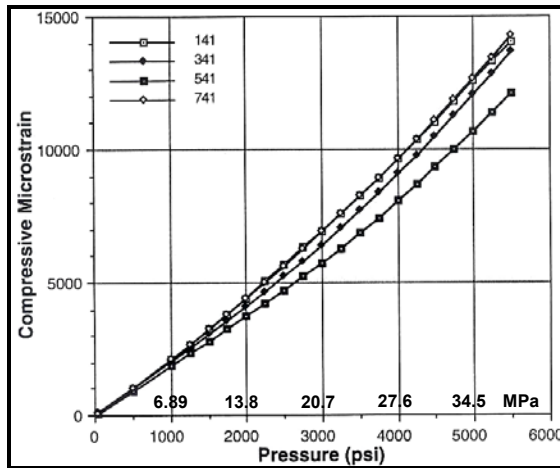


Figure 3.2 Axial strains at Bay 4-5, the area of failure initiation, exceeded  $-14000 \mu\text{strain}$  at 3 of 4 locations

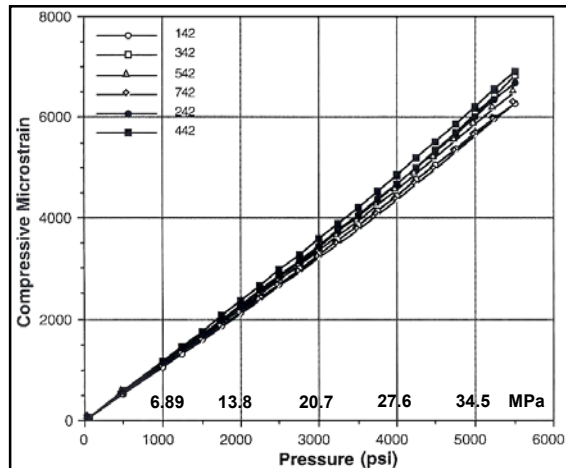


Figure 3.3 Hoop strains at Bay 4-5 approach  $-7000 \mu\text{strain}$  and show no evidence of buckling

The failure analysis strategy was to re-employ the cylinder finite element model to match the modeled strains with those measured in the hydrostatic collapse test, then to apply various failure criteria to the validated stresses and strains to quantify each criterion's ability to predict the failure location and test pressure.

### 4. UPDATING THE FINITE ELEMENT MODEL TO ACCURATELY REPRODUCE TEST STRAINS

The cylinder geometry is in Figure 4.1. Sample finite element model predictions (axial strains) are shown for a midbay/ring combination in Figure 4.2. Once the strain predictions most closely match the test strains, they become inputs to candidate failure criteria to evaluate each criteria's predicted failure location and pressure. Figure 4.3 tracks how the finite element model test strain predictions at 34.5 MPa (5000 psi) external loading improved updated based on more material tests or more innovative analyses that included residual stresses and nonlinearities.

The finite element model was first updated to the most accurate possible dimensions and laminate stacking sequence from leftover cylinder end rings and intact fragments from the tested cylinder. Strain results are compared with the test strains in Figure

4.1, bar 1 (“test strains”) and bar 2 (“Pressure only – no residual stress effects”), with disappointing variation, particularly in O.D. and I.D. midspan axial and hoop strains.

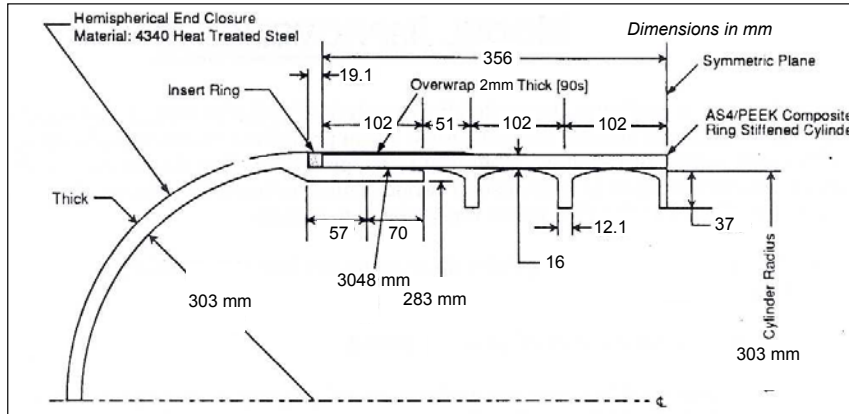


Figure 4.1 The cylinder featured a 2.27:1 hoop/axial ratio shell, five all-90° rings with full fillets, a 90° buildup at the shell extension outer diameter, and steel hemispherical end closures with tapered lands.

The finite element model was next updated with new moduli measured from leftover cylinder end rings and intact fragments (with what damage?) from the hydrostatically tested cylinder. This is the third bar in Figure 4.3, labelled “ply modulus modification – no residual stress effects.”

A critical upgrade to the cylinder finite element model was to account for the initial cylinder shape resulting from process-induced residual stresses. Although cylinder geometric deviations were seemingly small, for example a 0.25 mm (0.010 inch) reduction in midbay outer diameter, a significant improvement in predicted strain correlation with test strain data was achieved when including this initial shape effect. This in the fourth bar in Figure 4.3 labelled “Pressure only with residual stress effects.”

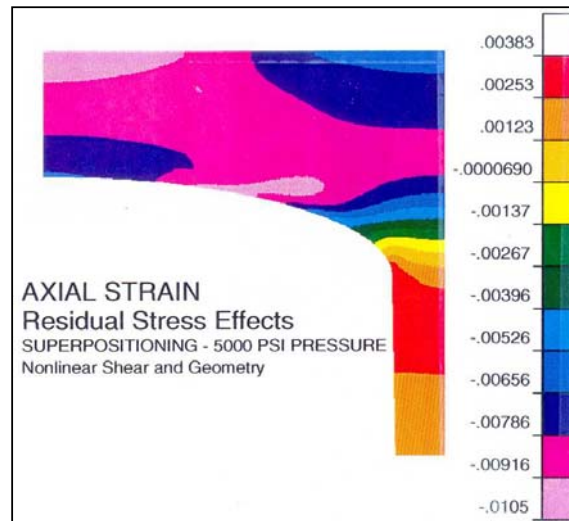


Figure 4.2 Axial strain contour for final analysis case at 34.5 MPa (5000 psi) external hydrostatic pressure load.

The final critical upgrade to the cylinder finite element model was to account for the significant material non-linearity in the transverse shear direction on the ply level. An incremental loading strategy was developed whereby piecewise linear increments in the stress-strain response were superimposed throughout the loading history to generate the non-linear shear behavior of the cylinder circumferential ring fillets. Strain dependent element properties were based upon ply level constitutive relations. A new code, LAMPATNL, was developed for use with ABAQUS to incorporate nonlinear shear stress-strain material properties with finite element analysis [3].

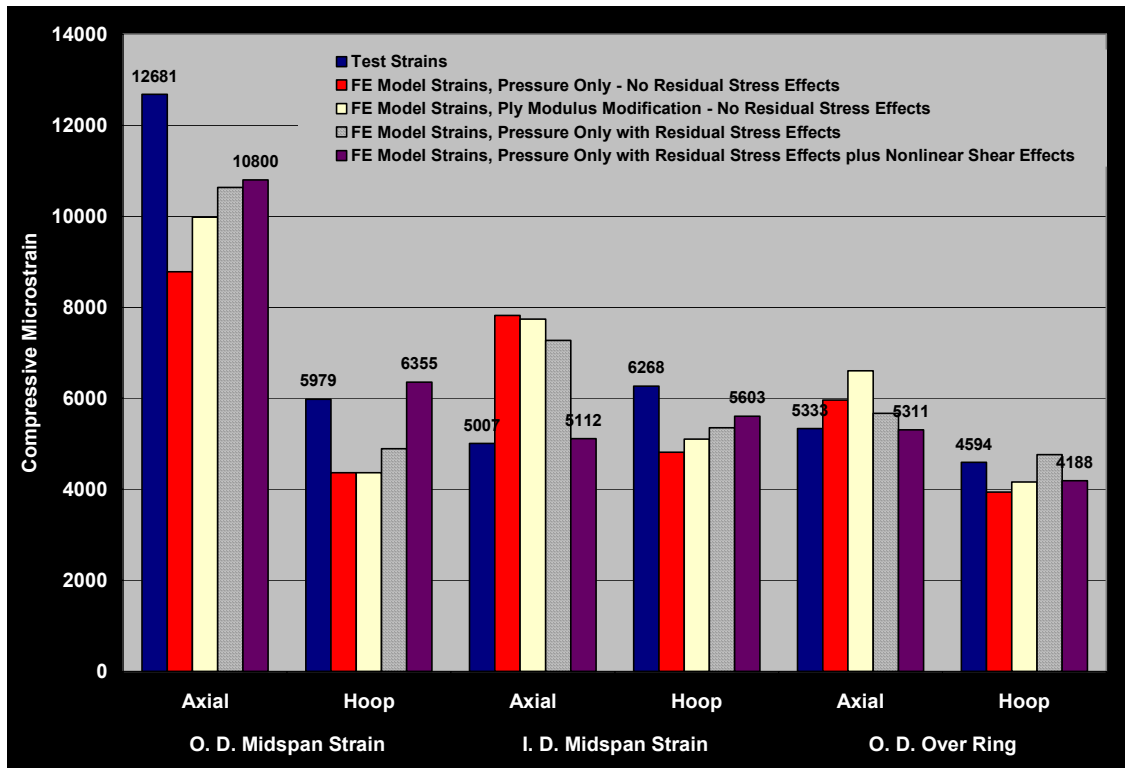


Figure 4.3 Test strains compared with strain predictions from the finite element model, including: 1<sup>st</sup> - test strains, 2<sup>nd</sup> - pressure only, 3<sup>rd</sup> - with modulus modifications, 4<sup>th</sup> - with residual stress effects, and 5<sup>th</sup> - additionally with non-linear shear.

Using all the above improvements (best dimensions, best properties, actual residual stress induced shape, non-linearities,) the maximum percentage error for all predictions was 14.8% comparing with the test data. This particular value was higher than hoped for, but fit the data best when considering the other strain values in other directions. Other axial strains were within 2.1%; hoop strains within 10.9%.

## 5. FAILURE CRITERIA APPLIED TO PREDICTED STRAIN

Four failure criteria were applied to the predicted strains from the cylinder midbay finite element model. It was found that knowledge of the in situ transverse interlaminar shear strength,  $S_{23}$ , was critical to the use of each criterion. When  $S_{23}$  was set equal to the short beam shear strength, 35.16 MPa (5.1 ksi), predictions indicated cylinder failure by shear in the fillet for both the Maximum Stress and Modified-Hashin failure criteria. Much better predictions occurred with  $S_{23}$  set equal to half the axial compression strength, i.e.  $\frac{1}{2}X_{22c}$ , or 91.7 MPa (13.3 ksi). In that case, the Maximum Stress, the Maximum Strain, and the Modified Hashin criteria all predicted the correct axial midbay OD failure location and axial compression failure mode with essentially the same pressure, ranging from 34.16 to 35.51 MPa (4955 to 5150 psi). The higher value is only 6% below the actual collapse test pressure.

## CONCLUSIONS



The filament wound/tape placed cylinder was hydrostatically tested and failed within 3% of the pre-test prediction. The failure mode was axial collapse away from the hemispherical ends. The “building block approach” applied in the cylinder development aided establishing design allowables as an integral step in process proveout. For the failure analysis, strain predictions were updated after the test with actual cylinder and ring dimensions, modulus measurements, and new analyses that accounted for (1) residual stresses and the initial pre-test cylinder shape that developed during process cool-down and (2) non-linear shear in the ring fillets. The Maximum Stress and Modified Hashin criteria predicted ring failure when  $S_{23}$  was set equal to its test value (ignoring the potential synergistic benefit of compression upon shear). The Maximum Stress, Maximum Strain, and Modified Hashin failure criteria all predicted the correct axial collapse failure when  $S_{23}$  was set higher, equal to  $\frac{1}{2}$  the shell axial compression strength.

### ACKNOWLEDGEMENTS

The authors acknowledge the contributions of many co-investigators. Jay Sloan, DuPont Engineering, led the failure analysis. Kent Tacey, Dave Bonnani, Wayne Phyllaier, and Bob Rockwell, Naval Surface Warfare Center, Carderock Division, assisted throughout the failure analysis effort. Travis Bogetti, U. S. Army Ballistics Research Laboratory, developed the nonlinear material constitutive modelling capability. Professor Jack Gillespie, University of Delaware, consulted throughout the failure analysis and led the innovative post collapse test material evaluations. Mike Smoot led the cylinder fabrication. Brian Waibel, Accudyne Systems, created color animations of the cylinder deflection sequence.

### REFERENCES

- [1] LAMONTIA, M. A., M. B. GRUBER, J. F. PRATTE, “The Fabrication and Performance of Ring-stiffened Cylinders Manufactured by a Combined In Situ Automated Thermoplastic Filament Winding and Tape Laying Process,” Proceedings of the 25<sup>th</sup> Jubilee International SAMPE EUROPE Conference 2004 of the Society for the Advancement of Materials and Process Engineering, Paris EXPO, Porte de Versailles, Paris, France, March 30 – April 1, 2004, p.527.
- [2] LAMONTIA, M. A., M. B. GRUBER, M. A. SMOOT, J. G. SLOAN, and J. W. GILLESPIE, JR., “Performance of a Filament Wound Graphite/Thermoplastic Composite Ring-Stiffened Pressure Hull Model,” Journal of Thermoplastic Composite Materials, Vol. 8, January 1995, p.15.
- [3] TRAVIS A. BOGETTI; BRUCE P. BURNS; CHRISTOPHER P. HOPPEL; “LAMPAT: A Software Tool for Analyzing and Designing Thick Laminated Composite Structures,” Army Research Lab - Aberdeen Proving Ground MD Report Number A357103, September 1995.